AD-A124 453 TUNNELING SPECTROSCOPY AS A PROBE OF ADSORBATE-SURFACE INTERACTION(U) CALIFORNIA UNIV SANTA BARBARA DEPT OF PHYSICS P K HANSMA FEB 83 TR-14 N00014-78-C-0011 1/1

UNCLASSIFIED F/G 7/4 NL

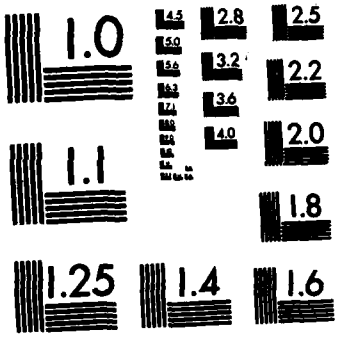

(12)

OFFICE OF NAVAL RESEARCH
Contract N0014-78-C0011, NR
Task No. NR056-673
Technical Report 14

# Tunneling Spectroscopy as a Probe of Adsorbate-Surface Interaction

by

Paul K. Hansma

Prepared for Publication
in
Journal of Electron Spectroscopy

(Presented at)

Third International Conference
"Vibrations at Surfaces"
Pacific Grove, CA
September 1-4, 1982

Department of Physics
Quantum Institute
University of California
Santa Barbara, CA



February, 1983

SECURITY CLASSIFICATION OF THIS PAGE *(When Data Entered)*

| REPORT DOCUMENTATION PAGE | | READ INSTRUCTIONS BEFORE COMPLETING FORM |
|---|---|---|
| 1. REPORT NUMBER | 2. GOVT ACCESSION NO. A124453 | 3. RECIPIENT'S CATALOG NUMBER |
| 4. TITLE *(and Subtitle)* Tunneling Spectroscopy as a Probe of Adsorbate-Surface Interactions | | 5. TYPE OF REPORT & PERIOD COVERED Technical |
| | | 6. PERFORMING ORG. REPORT NUMBER |
| 7. AUTHOR(s) P. K. Hansma | | 8. CONTRACT OR GRANT NUMBER(s) N0014-78-C-0011 |
| 9. PERFORMING ORGANIZATION NAME AND ADDRESS Department of Physics, Quantum Institute, University of California, Santa Barbara, CA 93106 | | 10. PROGRAM ELEMENT, PROJECT, TASK AREA & WORK UNIT NUMBERS NR056-6731 |
| 11. CONTROLLING OFFICE NAME AND ADDRESS Office of Naval Research Department of the Navy Arlington, VA 22217 | | 12. REPORT DATE February, 1983 |
| | | 13. NUMBER OF PAGES 6 |
| 14. MONITORING AGENCY NAME & ADDRESS*(if different from Controlling Office)* | | 15. SECURITY CLASS. *(of this report)* Unclassified |
| | | 15a. DECLASSIFICATION/DOWNGRADING SCHEDULE |

16. DISTRIBUTION STATEMENT *(of this Report)*

Approved for public release and sale; distribution unlimited

17. DISTRIBUTION STATEMENT *(of the abstract entered in Block 20, if different from Report)*

18. SUPPLEMENTARY NOTES

19. KEY WORDS *(Continue on reverse side if necessary and identify by block number)*

Tunneling Spectroscopy, Vibrational Spectra, Tunnel Junction, Adsorbate-Surface Interactions, Top Metal Electrode, Inelastic Channel, Benzyl-$d_7$, Aluminum, IR, Raman

20. ABSTRACT *(Continue on reverse side if necessary and identify by block number)*

Tunneling spectroscopy is a sensitive probe of two classes of adsorbate-surface interactions: interactions of the adsorbate with the substrate on which it is adsorbed and adsorbate interactions with the top metal electrode that is evaporated on top of it. The talk by Professor Hipps focuses on the first of these classes. This talk focuses on the second. In general, the interaction of the adsorbed molecules with the top metal (over)

DD FORM 1 JAN 73 1473 EDITION OF 1 NOV 65 IS OBSOLETE
S/N 0102-LF-014-6601

SECURITY CLASSIFICATION OF THIS PAGE *(When Data Entered)*

electrode produces a down-shift in the vibrational mode position ranging in size from $\lesssim$ 0.1% to $\lesssim$ 10% depending on the dipole derivative of the mode and the type of top metal electrode.

# TUNNELING SPECTROSCOPY AS A PROBE OF ADSORBATE-SURFACE INTERACTIONS

PAUL K. HANSMA

Department of Physics, University of California, Santa Barbara, CA 93106 USA

## ABSTRACT

Tunneling spectroscopy is a sensitive probe of two classes of adsorbate-surface interactions: interactions of the adsorbate with the substrate on which it is adsorbed and adsorbate interactions with the top metal electrode that is evaporated on top of it. The talk by Professor Hipps focuses on the first of these classes. This talk focuses on the second. In general, the interaction of the adsorbed molecules with the top metal electrode produces a down-shift in the vibrational mode position ranging in size from $\leq$ 0.1% to $\leq$ 10% depending on the dipole derivative of the mode and the type of top metal electrode.

## INTRODUCTION

Tunneling spectroscopy measures the vibrational spectra of molecules adsorbed in a tunnel junction. It can be understood with a simple analogy. Fig.

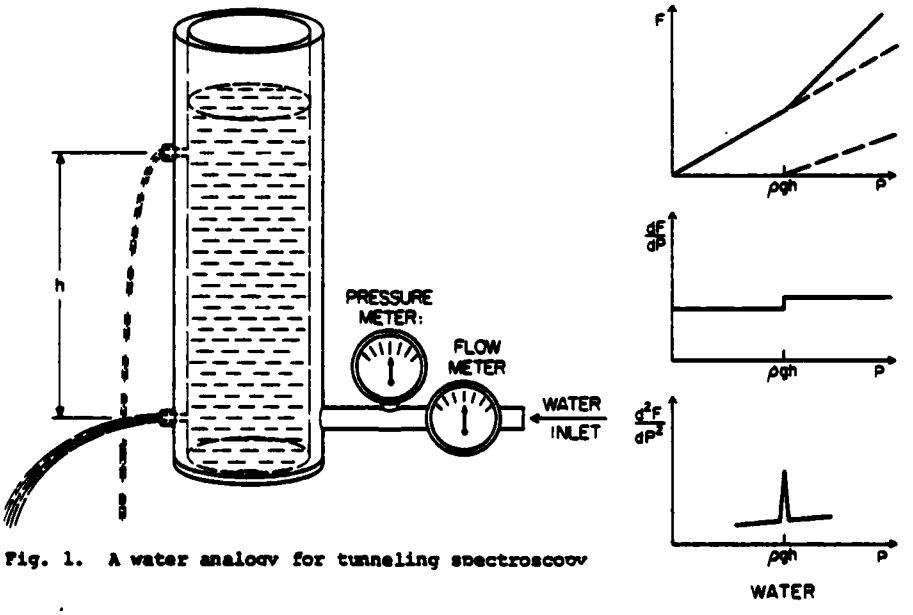


Fig. 1. A water analogy for tunneling spectroscopy

1 shows a container of water with two holes. As the pressure is increased, the height of water in the container increases and the flow increases. As shown in the plot of the flow, F, versus the pressure P, when the pressure reaches ρgh, the water reaches the upper opening, and the flow has a kink upwards. This kink becomes a step in the first derivative and a peak in the second derivative. Thus, even if the column were covered with a black cloth, the height of the hole could be determined at a position of the peak in the lowest graph: specifically, the height of the hole would be equal to the pressure at which the step occurred divided by ρg.

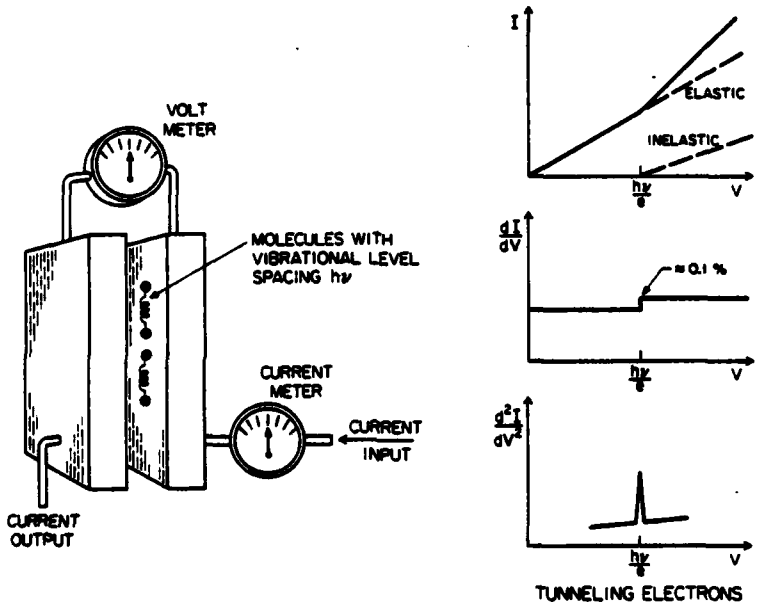


Fig. 2. The molecular vibration energy hν is revealed as a peak in the tunneling spectrum at hν/e.

Fig. 2 contains a schematic view of a tunnel junction. In this case, the current through the tunnel junction is measured as a function of the voltage across it. As the voltage is increased, the current shows a kink at hν/e. At this voltage, the most energetic tunneling electrons, with energy eV, have just enough energy to excite the molecules. Below this voltage the molecules will contribute to the tunneling barrier and perhaps decrease the elastic conductance by two orders of magnitude. Above this voltage, a very small percentage of the lost conductance is regained by the opening of an inelastic tunneling

channel in which the electron excites the molecule and then continues to tunnel across. Unfortunately, the conductance increase due to the opening of the inelastic channel is typically only a tenth of a percent so that the 2nd derivative spectrum shown in the lower trace must be obtained to see the structure.

Fig. 3 shows a real tunneling spectrum from some recent work by Atiye Bayman, et al. (ref.1). Note that there are many peaks. Many elastic tunneling channels open up because there are many vibrational modes of this relatively complex molecule. In general, we find that Raman active and infrared active modes are present with comparable intensities in tunneling spectra (refs. 2,3, 4) and that there is a small orientational preference toward modes vibrating perpendicular to the oxide surface (ref. 5).

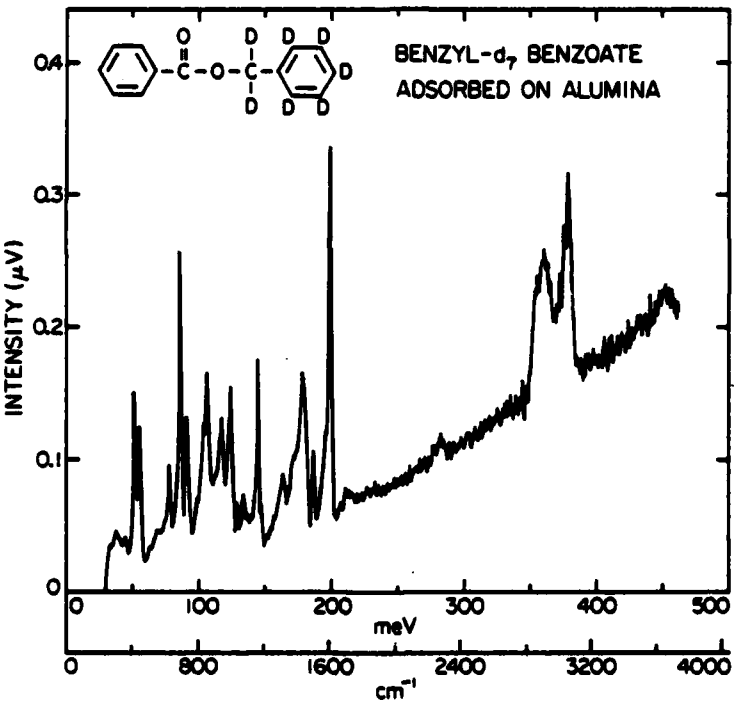


Fig. 3. A typical tunneling spectrum has many corresponding to many vibrations.

Tunneling spectroscopy is a powerful probe of chemisorption. For example, in this case, from the near absence of a C-D stretching peak near 280 meV and the correspondence with a benzoate ion spectrum, we conclude that this molecule

predominantly dissociates: the benzyl-$d_7$ part leaves the surface and the remaining part ponds as benzoate ions. Professor Hipps, in his talk, will give other examples of the interesting adsorbate-surface interactions that can be observed between adsorbed molecules and the substrate on which they are being adsorbed. This talk will focus on the adsorbate-surface interactions that can be observed between the adsorbed molecules and the top metal electrode that is evaporated onto them.

## EXPERIMENTAL TECHNIQUES

Fig. 4 is a schematic view of tunnel junction fabrication. An aluminum strip is evaporated onto a substrate through a mask, it is oxidized in air or

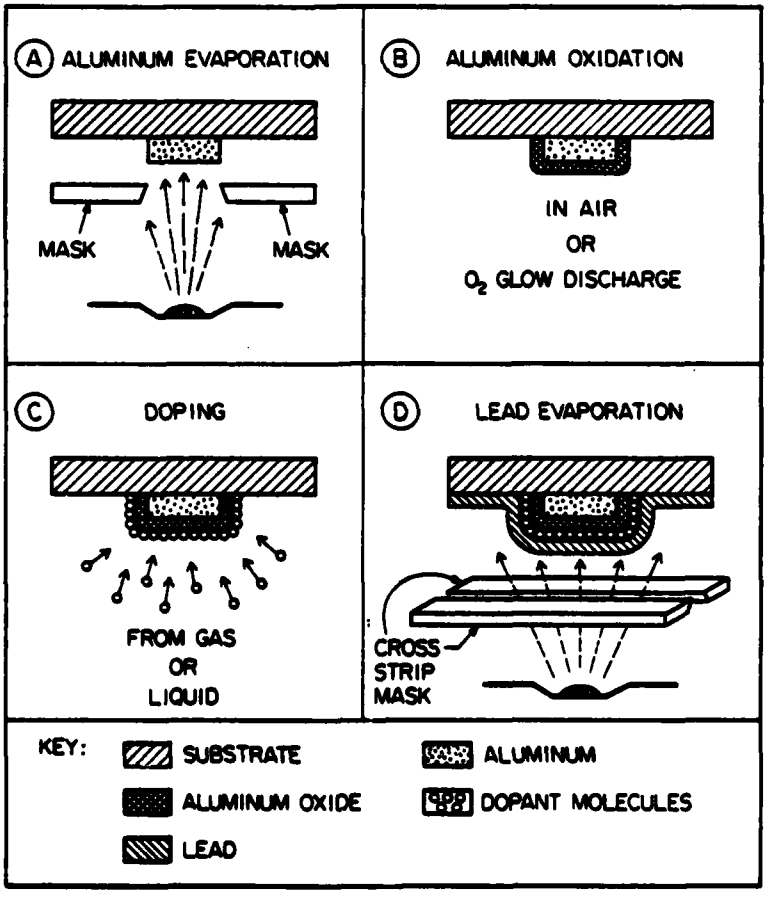


Fig. 4. Tunnel junction fabrication.

oxygen glow discharge, it is doped with a monolayer of molecules from the gas phase or from a liquid solution and the junction is completed with a cross strip of evaporated metal, usually lead. It is the interaction of the dopant molecules with this top metal electrode that is the focus of this paper.

## EXPERIMENTAL RESULTS

Fig. 5 shows a differential tunneling spectrum (ref. 6) of benzoate ions adsorbed on alumina. (A differential tunneling spectrum is simply a different spectrum between a doped and an adjacent undoped junction on the same substrate. This eliminates some of the background and impurity peaks.) John Kirtley studied this ion in order to see the vibrational mode shifts due to the evaporated top metal electrode (ref. 7). As an example of his work, let us focus our

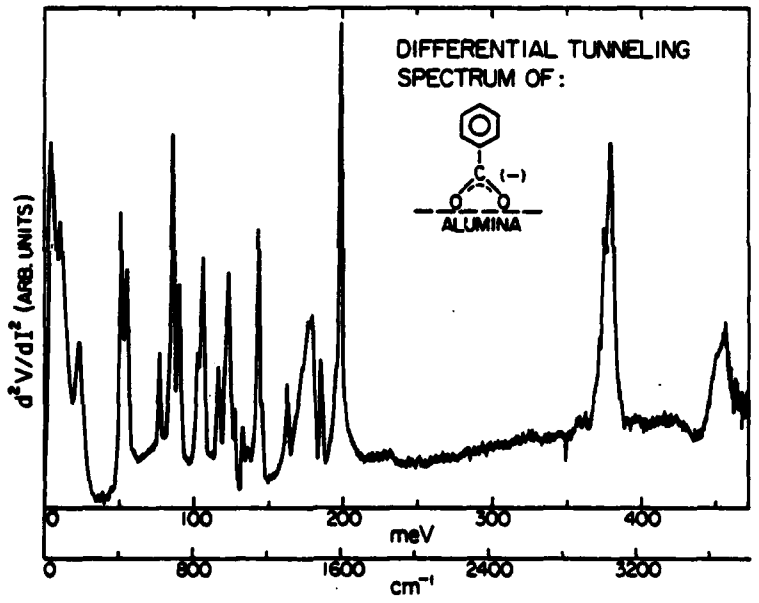


Fig. 5. The sharp peak near 1600 $cm^{-1}$ was among those studied for peak shifts due to the top metal electrode by Kirtley, et al. (ref. 7).

attention on the large, sharp peak near 1600 $cm^{-1}$. How much has this peak shifted from the position that would be found with optical spectroscopy of benzoate ions and no top metal electrode? Fig. 6 shows Dr. Kirtley's results (ref. 7) for that peak. The curve with circles shows the position of the peak in a tunneling spectrum with a silver top electrode; the curve with triangles

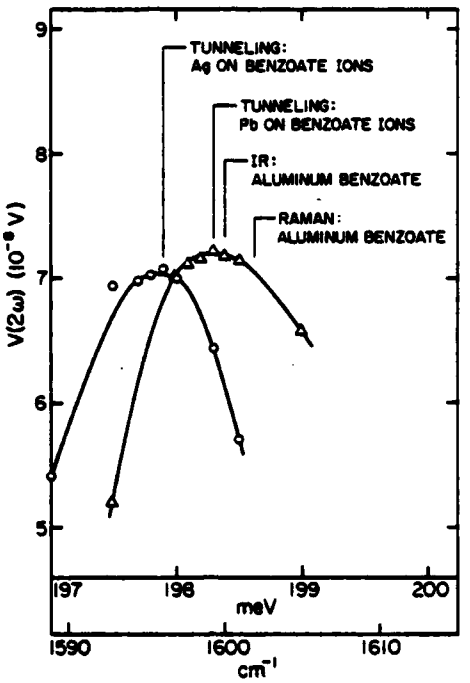


Fig. 6. Expanded view of the sharp peak near 1600 $cm^{-1}$ from Fig. 5 for different top metal electrodes.

shows the position of the peak in a tunneling spectrum with a lead top electrode. The lines show the IR and Raman positions of the peak for aluminum benzoate. It should be pointed out that the IR and Raman are measuring the same peak. The fact that their positions differ indicates the uncertainty in these measurements. If we assume that the actual position for aluminum benzoate is the average of the IR and Raman values, then we obtain a shift due to the top metal electrode in tunneling of about two wavenumbers out of 1600 $cm^{-1}$ or about 0.13%. The down-shift in going to a silver electrode is another three wavenumbers or about 0.2%. Fig. 7 summarizes peak shifts for a number of vibrational modes (refs. 7,8,9). Note that the shifts are large for C-O and O-H vibrational modes.

Fig. 8 shows Dr. Kirtley's results for O-H and O-D vibrational modes with lead and gold top electrodes (ref. 8). Here we see those much larger peak shifts. We can also note that peaks are broadened with the gold top electrode.

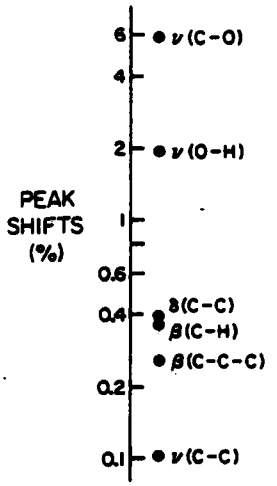


Fig. 7. Peak shifts due to the top metal electrode depend on the type of vibrational mode.

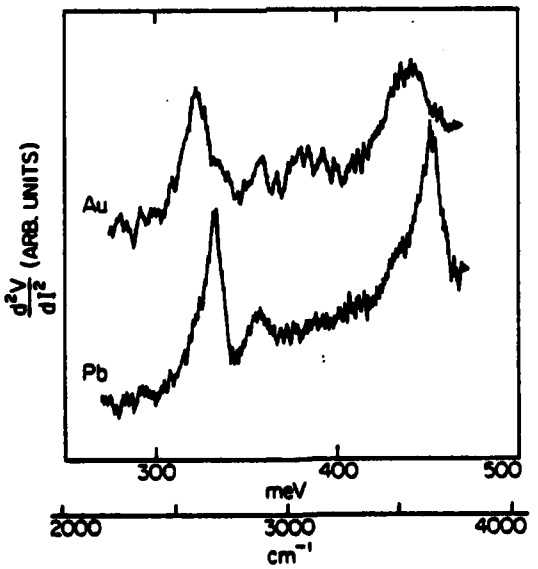


Fig. 8. The relatively large peak shifts for O-H and O-D groups can be easily seen (ref. 8).

Fig. 9 shows the C-O vibrational modes for which the largest peak shifts yet measured have been found (ref. 9). The figure compares an inelastic electron spectrum with a lead top electrode to infrared results (ref. 11) and electron energy loss results (ref. 10). The peak shifts here are roughly 4% for the higher energy C-O stretching mode and 8% for the lower energy C-O stretching mode.

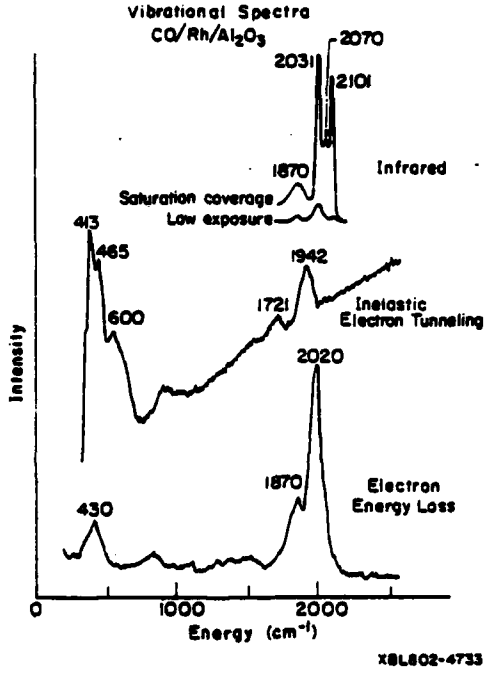


Fig. 9. These three techniques for vibrational spectroscopy complement one another (ref. 10).

This type of junction proves difficult to make with different top electrodes but some results obtained by Dr. Bayman (ref. 12) are shown in Fig. 10. In this case, a thallium top electrode gave peak positions similar to that for lead, while tin and indium top electrodes seem to have eliminated the species with the lower energy C-O stretching vibration and correspondingly modified the low energy part of the vibrational spectrum. Her work contains more extensive results for CO on iron/alumina where again relatively small peak shifts are seen

in the C-O stretching region and profound modification of the structure in the low energy region is found.

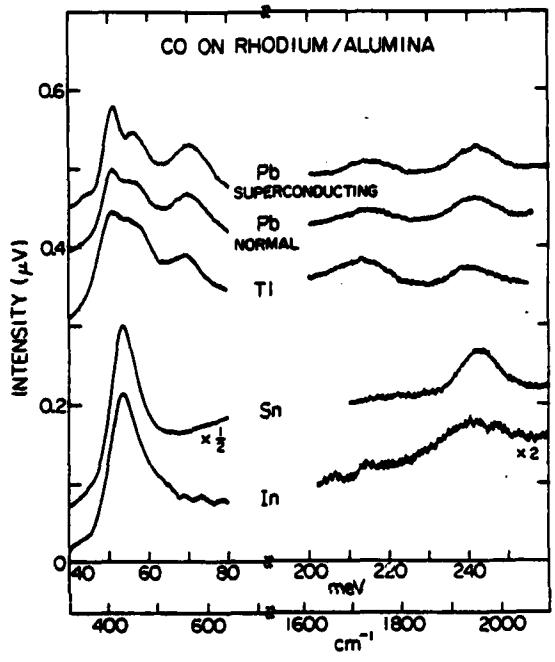


Fig. 10. More dramatic top electrode effects are found for CO on supported metal particles (ref. 12).

DISCUSSION

These experimental results can be understood within the framework of a theory developed by Dr. Morawitz (ref. 13) and later generalized by Morawitz and Philpott (ref. 14) and others. In these theories, the primary interaction is between the oscillating dipole mode and the image in the metal surface. The end result is that the shift $\Delta\omega_{\perp}$, for a dipole oscillating perpendicular to the surface, is:

$$\Delta\omega_{\perp} = \frac{-q_1^2}{8m\omega_0 n_1^2 d^3}\left\{1 + \frac{3}{2}\beta\frac{q_0}{q_1}\left[1-\left(1+\frac{a}{2d}\right)^{-2}\right]\right\} \qquad (1)$$

For oscillations parallel to the surface

$$\Delta\omega_{\parallel} = -q_1^2/16m\omega_0 n_1^2 d^3 \qquad (2)$$

Here, $Q_1$ is the dipole derivative, m is the oscillating mass, $\omega_0$ is its unperturbed frequency, $n_1$ is the real index of refraction of the oxide, d is the effective distance to the metal surface, $\beta$ is the exponential fall-off constant of the Morse potential, $\beta = (\omega_0^2 m/2E_D)$, $Q_0$ is the static dipole moment and a is the bond length (Equation from ref. 7).

It is the dependence on $Q_1$ and d that can be used to understand the data presented in this paper semiquantitatively: only semiquantiatively because we cannot measure d directly. We can, however, use d as a fitting parameter and ask if the values are reasonable. For example, if we assume that the O-H stretching mode without the top electrode should occur near 455 mev as observed with infrared spectroscopy, we find that the shift down to 446 mev observed with the top lead electrode implies $d = 0.8$ Å. (Here we have taken $Q_0 = 0.71$ e, $Q_1 = 0.32$ e, $m = m_p$, $n_1^2 = 3$, $\beta = 1.6 \times 10^8$ $cm^{-1}$, as in ref. 7.) This is certainly in the ball park for the parameter. Further, the observation that a gold top electrode gives a larger downshift can be understood. Gold has a smaller radius than lead and so presumably it would come closer to the oscillating dipole.

The much smaller shifts for hydrocarbon vibrations can also be understood. The major differences are that the hydrocarbon dipole derivatives are much smaller, typically $Q_1 \lesssim 0.1$ e (refs. 5,7) and the effective distance to the vibrational modes, at least for a large molecule, is larger. Similarly, the larger shifts for C-O vibrations can be understood, since $Q_1$ is extremely large for these vibrations. Though the value differs with the type of adsorbed CO and from metal to metal (ref. 9), a value of order $Q_1 = 2$ e is typical and fits the data with the same d as for O-H vibrational shifts.

It should be emphasized, however, that these fits are only semiquantitative. True quantitative comparison will depend on independent methods for measuring d.

The final figure presents an interesting confirmation of the rough ideas presented in this paper. It shows a single junction spectrum of hexanoic acid on alumina, a spectrum from an undoped control junction, and their differential spectrum. Note that the position of the O-H vibration is higher on the doped junction than on the control. In fact, the position on the doped junction, 453 meV, is very close to the position for O-H groups on alumina with no top metal electrode, 455 ± 3 meV (ref. 8). Perhaps this can be understood with the following simple model. The hexanoic acid monolayer separates the top metal electrode from the O-H groups by distances of several Å. Since the distance dependence of the theory of Morawitz, et al. is more rapid than $d^2$, this spacer layer will very much reduce the peak shifts of the O-H group due to the top metal electrode. Thus, we would expect the O-H peak at higher energy in doped compared to undoped junctions.

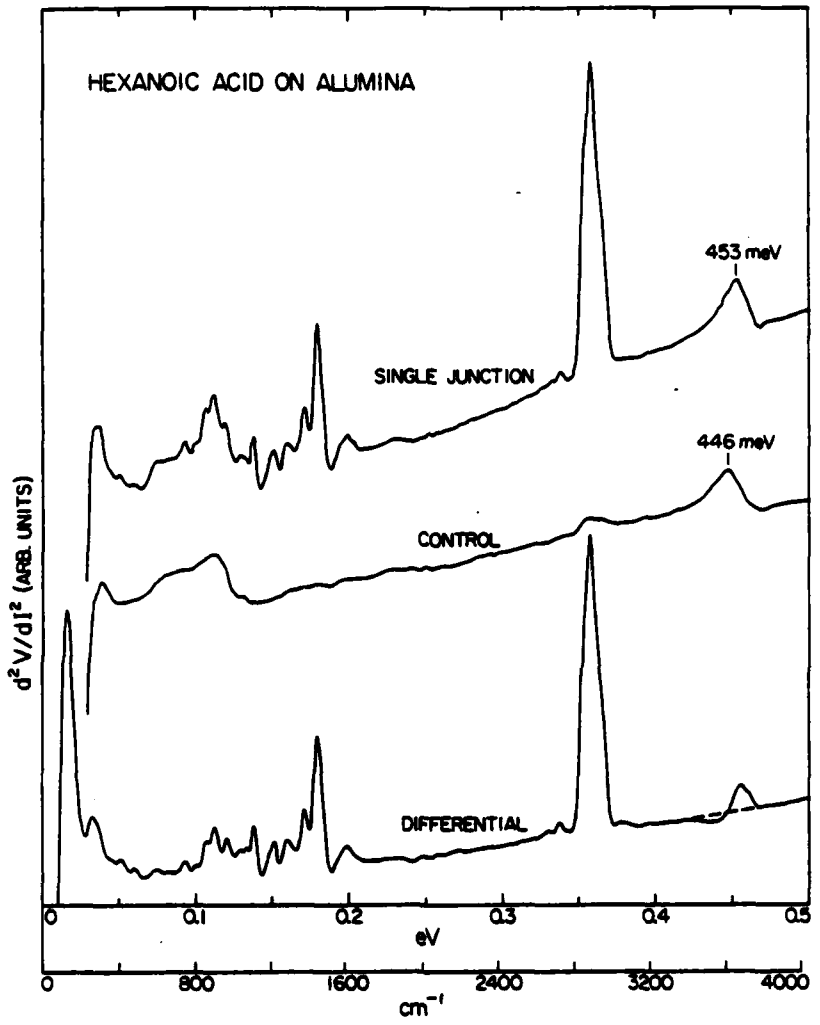


Fig. 11. The O-H down-shift from s 455 meV for no top electrode is reduced for a doped junction.

This up-shift in O-H group of doped junctions (or, perhaps more properly, decrease in the down-shift) is very characteristically seen in differential tunneling spectrum as a dip followed by a peak in the O-H region as shown in the bottom trace of Fig. 11. If you review Fig. 5, you will see a similar structure in the O-H region there.

## CONCLUSIONS

1. Vibrational mode shifts due to the top metal electrode in tunneling spectroscopy can be observed by comparison of tunneling spectra with infrared, Raman and electron energy results without the top electrode and by intercomparison of tunneling spectra with different top electrodes.

2. The magnitude of the peak shifts ranges from an order of a tenth of a percent for hydrocarbon vibrations to as large as many percent for O-H and C-O vibrations.

3. The shifts can be semiquantitatively understood within the framework of an image dipole theory developed by Morawitz, et al.

4. Quantitative confirmation will depend upon the accurate, independent determination of the effective distance to the top metal electrode.

## ACKNOWLEDGEMENTS

This work was supported in part by NSF Grant DMR79-25430 and the Office of Naval Research. I am grateful to J. Kirtley, J. Hall, R. Kroeker and A. Bayman for helping me understand the results presented here.

## REFERENCES

1. A. Bayman, P. K. Hansma and L. H. Gale, Surf. Sci. submitted.
2. K. W. Hipps, U. Mazur and M. S. Pierce, Chem. Phys. Lett. 68 (1979).
3. W. H. A. Weinberg, Rev. Phys. Chem. 29 (1978) 115-139.
4. P. K. Hansma, Phys. Reports 30C (1977) 145-206.
5. J. Kirtley and J. T. Hall, Phys. Rev. B 22 (1980) 848-856.
6. S. Colley and P. K. Hansma, Rev. Sci. Instr. 48 (1977) 1192-1195.
7. J. Kirtley and P. K. Hansma, Phys. Rev. B 13 (1976) 2910-2917.
8. J. Kirtley and P. K. Hansma, Phys. Rev. B 12 (1975) 531-536.
9. R. M. Kroeker, W. C. Kaska and P. K. Hansma, J. Catal. 57 (1979) 72-79.
10. L. H. Dubois, P. K. Hansma, and G. A. Somorjai, Appl. of Surf. Sci. 6 (1980) 173-184.
11. J. T. Yates, Jr., T. M. Duncan, S. D. Worley and R. W. Vaughn, J. Chem. Phys. 70 (1979) 1219-1224.
12. A. Bayman, P. K. Hansma and W. C. Kaska, Phys. Rev. B 24 (1981) 2449-2455.
13. H. Morawitz, Phys. Rev. 187 (1969) 1792.
14. H. Morawitz and M. R. Philpott, Phys. Rev. B 10 (1974) 4863.

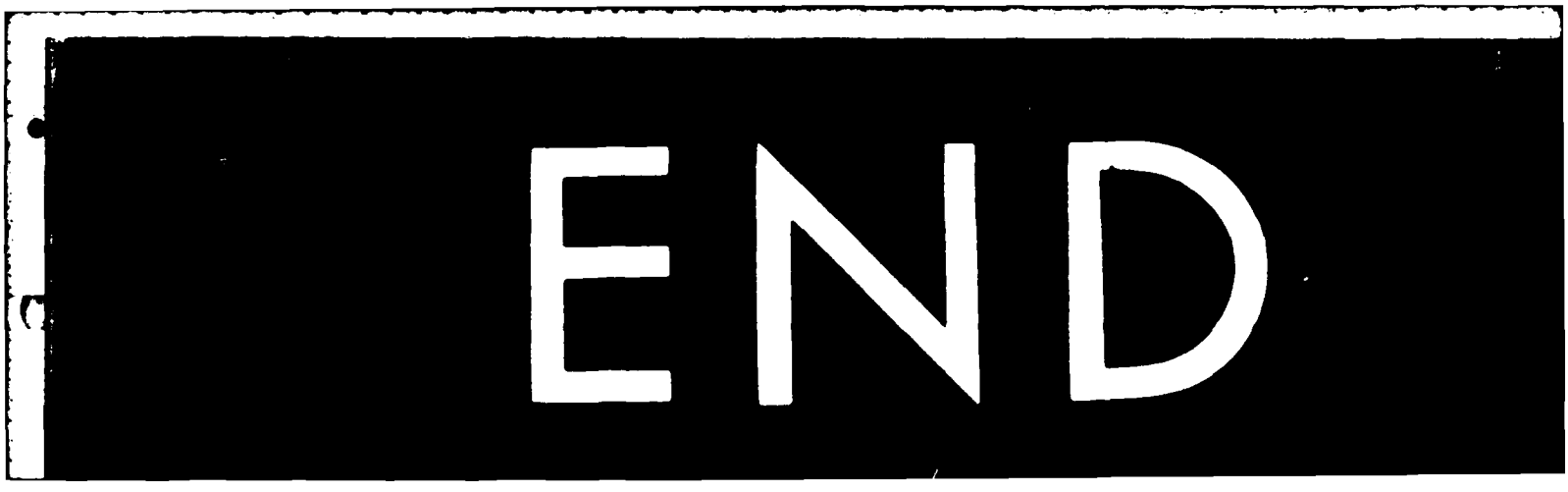
END